



## KINETICS, ISOTHERMS AND THERMODYNAMICS STUDIES OF SORPTION OF $\text{Cu}^{2+}$ ONTO NOVEL ZEROVALENT IRON NANOPARTICLES

By

A.O. Dada<sup>1\*</sup>,

F.A. Adekola<sup>2</sup>

&

E.O. Odebumi<sup>3</sup>

<sup>1\*</sup>Department of Physical Sciences  
(Industrial Chemistry Programme),  
Landmark University,  
Omu-Aran, Kwara State, Nigeria.

<sup>2</sup>Department of Industrial Chemistry,  
University of Ilorin, Nigeria.

<sup>3</sup>Department of Chemistry,  
University of Ilorin, Nigeria.

\*Corresponding authors: dada.oluwasogo@lmu.edu.ng

**Abstract:** A novel nano-scaled zerovalent iron (nZVI) is an effective adsorbent for scavenging inorganic and organic toxicants. nZVI was synthesized in a single pot system using bottom-up approach and were characterized by BET, SEM, EDX and FTIR. In this study, sorption of  $\text{Cu}^{2+}$  onto nZVI was carried out vis-à-vis the investigation of physicochemical parameters (initial metal ion concentration, pH, temperature, adsorbent dose) at 298 K. The sorption data obtained at optimum conditions were subjected to six different isotherm models (Langmuir, Freundlich, Tempkin, Dubinin-Raduskevich (DRK), Halsey and Harkin-Jura). However, the equilibrium sorption data were best described by both Langmuir and Temkin isotherm models with Langmuir maximum monolayer coverage ( $Q_{max}$ ) of 40.816 mg/g and regression correlation value ( $R^2 > 0.96$ ) supporting a chemisorption mechanism. Pseudo first-and second-order, Elovich, fractional power and intra-particle diffusion models were applied to the adsorption data in order to investigate the kinetic process; pseudo-second order fitted the data most. The intra-particle diffusion model suggested that the intra-particle diffusion was one of the rate-limiting steps. The values of the Gibbs free energy showed the feasibility and spontaneity of the sorption process. The

removal efficiency of  $\text{Cu}^{2+}$  (> 98%) onto zerovalent iron nanoparticles revealed that nZVI is a promising and efficient adsorbent that can be utilized by industries on a large scale for waste treatment.

**Keywords:** Zerovalent Iron nanoparticles; Sorption; Isotherms; Kinetics and Thermodynamics

## Introduction

Copper is transition metal and one of the heavy metals in group 1B with density of  $8.9 \text{ g.cm}^{-3}$ . It is released into the environment through natural phenomena and anthropogenic activities and these account for its wide spread in the environment. Copper is often found near mines, industrial settings, landfills and waste disposals. Most copper compounds will settle and be bound to either water sediment or soil particles. Soluble copper compounds form the largest threat to human health. Usually, water-soluble copper compounds occur in the environment after release through application in agriculture. Copper in the blood exists in two forms either bound to *ceruloplasmin* or the rest "free", loosely bound to albumin and small molecules. Free copper causes toxicity, as it generates reactive oxygen species such as superoxide, hydrogen peroxide and the hydroxyl radicals all of which damage proteins, lipids and DNA [1]. There are a number of adverse effects of copper due to over-exposure such as: irritation of the nose, mouth and eyes, headaches, stomachaches, dizziness, vomiting, *hematemesis*, diarrhea, hypotension, melena, coma, jaundice. Intentionally, high uptakes of copper

may cause liver and kidney damage and even death [2].

Nanoparticles are the new trend of effective adsorbents used in the decontamination of water and immobilization of heavy metal ions from their solutions. Research on the utilization of nanoparticles is on the increase due to their special characteristics. Various methods have been reported by researchers for the removal of heavy metal ions from the environments such as chemical precipitation [3], ion exchange [4], solvent extraction [5], ultra-filtration [6], reverse osmosis [7], cementation [8], electro-dialysis [9]. These methods are not economical and have many disadvantages such as incomplete metal removal, high reagent and energy consumption, and generation of toxic sludge or other waste products that require disposal or treatment. In contrast, the adsorption technique is one of the preferred methods for the removal of heavy metal ions because of its efficiency and low cost [10].

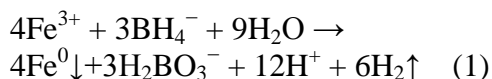
Although, previous researchers have investigated the removal of copper ions by utilizing natural clinoptilolite [11], amino-functionalized magnetic nanoparticles [12], pectin-iron oxide magnetic nanocomposite [13], Carboxymethyl-cyclodextrin conjugated magnetic nanoparticles

[14], polymer nanofibrous materials [15], titanate nanotubes [16], and palm shell activated carbon [17] yet to our knowledge, sorption of copper onto nZVI has not been the subject of detailed studies. The main objective of this research is to investigate the kinetics, isotherms and thermodynamics of sorption of copper ions onto core zerovalent iron nanoparticles vis-à-vis the optimization of sorption physicochemical parameters (pH, contact time, initial copper ions concentration and temperature).

## Materials and Methods

### Synthesis of Zerovalent Iron nanoparticles

All the chemicals used are of analytical grade purchased from Sigma Aldrich, USA. The two precursors used for the synthesis of zerovalent iron nanoparticles are 0.023 M solution of Ferric Chloride and 0.125 M solution of NaBH<sub>4</sub> in the ratio 1:5 respectively following the procedure reported elsewhere in the literature [18, 19]. For better formation of nano-scale zerovalent Iron (nZVI), more of NaBH<sub>4</sub> solution is needed than Fe<sup>3+</sup> solution. As soon as the borohydride solution is added to Ferric chloride solution drop by drop in a glove box under inert environment. Ferric ion was reduced to zerovalent iron with an indication of a colour change according to the reaction:



The black particles of (nZVI) that appeared was further stirred for 3 h. nano-scale zerovalent Iron (nZVI) was separated from the solution using vacuum filtration apparatus and a cellulose nitrate membrane filter (Millipore filter) of 0.45 μm. nZVI was further washed with absolute ethanol three times and dried in a Genlab oven at 80 °C overnight.

### SEM/EDX, FTIR and BET

#### Characterization of the adsorbent:

The zerovalent iron nanoparticles were characterized by a combination of scanning electron microscopy and energy dispersive x-ray. The scanning electron microscopy (SEM) was used for the determination of the structural morphology; the quantitative elemental determination was done through the energy dispersive x-ray. The FTIR spectrum provided information about the local molecular environment on the surface of nZVI. The analysis on the determination of surface area, pore size and volume were performed using Brunauer-Emmett-Teller (BET) and Barrett-Joyner-Halenda (BJH) methods.

### Sorption Experiment

#### Batch Sorption Studies

The batch experiment was carried out following a similar procedure reported by Adekola *et al.* 2012 [20] and Dada *et al.* 2013 [21]. In a typical experiment, stock solution of 1000 ppm Cu<sup>2+</sup> was prepared by dissolving a calculated amount of CuSO<sub>4</sub>.5H<sub>2</sub>O (3.927g) in 1000 cm<sup>3</sup> of distilled deionized water in a standard

volumetric flask and serial dilution was made to prepare 10 – 100 ppm of the adsorbate. Batch sorption of  $\text{Cu}^{2+}$  ions onto nZVI was carried out and the sorption physicochemical parameters were determined. Generally, sorption experiment was done by contacting 100 mg of the nZVI with 50  $\text{cm}^3$  of different initial  $\text{Cu}^{2+}$  concentrations from 10ppm – 100 ppm in 60  $\text{cm}^3$  of Teflon bottle intermittently for 3 hours. The mixture was filtered and the filtrate was immediately analyzed for metal ions concentration using atomic absorption spectrophotometer (AAS) model AA320N at the Department of Physical Sciences, Industrial Chemistry Unit, Landmark University. The determination of the residual concentration using AAS was done in triplicate and the mean value for each set of the experiment was calculated. Optimization of sorption parameters (pH, contact time, adsorbent dose) was investigated following a similar procedure. Adsorption capacities were obtained using a mass balance equation [21]:

$$Q = \frac{(c_o - c_e)V}{m} \quad (2)$$

where Q is the equilibrium adsorption capacity per gram of nZVI ( $\text{mg g}^{-1}$ ), V is the volume of  $\text{Cu}^{2+}$  solution (L),  $C_o$  is the initial concentration of the  $\text{Cu}^{2+}$  solution before sorption ( $\text{mg L}^{-1}$ ),  $C_e$  is the final concentration of the  $\text{Cu}^{2+}$  solution after sorption ( $\text{mg L}^{-1}$ ), m is the mass in gram of nZVI. The removal efficiency was calculated

using the formulae in Eq. (3) as reported in the literature [22]

$$\% RE = \frac{C_i - C_e}{C_i} \times 100 \quad (3)$$

The adsorption data obtained from the optimized parameters were tested and analyzed using kinetics models (pseudo-first and pseudo-second order, Elovich, power factor and intra-particle diffusion) and six different isotherm models (Langmuir, Freundlich, Tempkin, Dubinin-Raduskevich, Halsey and Harkin-Jura)

### **Optimization of pH, Adsorbent Dose, Contact time and Initial $\text{Cu}^{2+}$ concentration**

The effect of pH, adsorbent dose contact time, initial  $\text{Cu}^{2+}$  concentrations were investigated to determine the optimum conditions. The effect of pH on sorption of  $\text{Cu}^{2+}$  onto nZVI was done by adjusting the pH using 0.1 M HCl and 0.1 M NaOH solutions. The effect of pH on the sorption of  $\text{Cu}^{2+}$  was carried out within the pH range of 1 – 7 that will not influence  $\text{Cu}^{2+}$  precipitation [23, 24].

The effect of adsorbent dose was carried out at optimum pH, contact time and initial concentration of 100  $\text{mg L}^{-1}$  and variable adsorbent doses of about 10 mg – 150 mg was contacted with 50  $\text{cm}^3$  portions of  $\text{Cu}^{2+}$  solution. The residual concentration was determined by AAS.

The effect of contact time on the sorption of Cu (II) ions onto nZVI was studied at various time intervals (0 – 120 min) at optimum pH and at different initial concentrations of 40 mgL<sup>-1</sup>, 60 mgL<sup>-1</sup>, 80 and 100mgL<sup>-1</sup>. 100 mg adsorbent dose of nZVI was agitated with 50cm<sup>3</sup> of the Cu(II) solution in 60 cm<sup>3</sup> Teflon bottle at the optimum conditions and the residual Cu<sup>2+</sup> concentration was determined in triplicate using AAS. The amount of metal ions sorbed was calculated using Eq. 2 and adsorption kinetics and mechanism were determined by data analysis using different kinetics models (pseudo first-order, pseudo second-order, Elovich, fractional power and intra-particle diffusion).

The effect of initial Cu<sup>2+</sup> ions concentration on the extent of uptake was investigated as reported in the literature [25]. This was done by agitating 100 mg of nZVI added into 50 cm<sup>3</sup> portions of Cu<sup>2+</sup> solutions within the range of 10 – 100 mgL<sup>-1</sup> on the orbital shaker at optimum time of 60 minutes. The amount of metal ions sorbed was calculated and the data were fitted into six different isotherm models such as: Langmuir, Freundlich, Temkin, Dubinin-Raduskevich (DRK), Halsey and Harkin-Jura.

## **Results and Discussion**

### **Characterization of Zerovalent Iron nanoparticles**

Table 1 shows the physiochemical parameters of zerovalent iron nanoparticles. The Point of zero charge (PZC) is defined as the pH at

which the surface of the adsorbent (nZVI) has a net neutral charge. The PZC of nZVI as determined by salt addition method is 5.28 (Fig not shown). The significance of this is that nZVI has a positive charge at solution pH values less than the PZC and thus a surface on which anions may adsorb. On the other hand, nZVI has a negative charge when the pH of the solution is greater than the PZC and thus be a surface on which cation may adsorb and thus the pH of nZVI is 5.28 indicating that nZVI better adsorption capacity was obtained at as solution pH greater than 5.28 stated on Table 1 [26].

The surface area by BET is 20.8643 m<sup>2</sup>/g, the t-Plot micropore area is 4.4140 m<sup>2</sup>/g which is lower than the t-Plot external surface area (is 16.4503 m<sup>2</sup>/g). These results revealed that most of the Cu<sup>2+</sup> ions are adsorbed at the external surface area and hence adsorption prevails. The large surface of nano-scaled zerovalent iron (nZVI) enhances its relevance in the waste water remediation [27].

The SEM micrograph of ZVI showed a spherical surface of chain-like, aggregated molecules. The chain-like aggregation is an indication of its magnetic property. The EDX spectrum of nZVI (Fig 1) showed the characteristics peaks of the nZVI, the information on the surface atomic distribution and the chemical elemental composition couple with the percentage composition of the prepared are stated on table 2. From table 2, iron (Fe) has the highest

atomic weight and atomic abundance of 86.47% and 51.28% respectively, this is in accordance with the report of [28, 29].

Figure 2 showed the FTIR spectrum of nZVI. The peaks on Fig. 2 are  $3345\text{ cm}^{-1}$ ,  $3256\text{ cm}^{-1}$ ,  $1632\text{ cm}^{-1}$ ,  $1328\text{ cm}^{-1}$ ,  $910\text{ cm}^{-1}$ , and  $686\text{ cm}^{-1}$ . The broad and intense peak around  $3345\text{ cm}^{-1}$ ,  $3256\text{ cm}^{-1}$  is due to the presence of O—H from alcohol used in washing nZVI to prevent rapid corrosion. The peak at  $1632\text{ cm}^{-1}$  may be attributed to H—O—H stretching of deionized deoxygenated water,  $1328\text{ cm}^{-1}$  corresponds to C—H bending,  $910\text{ cm}^{-1}$  is due to C—H bending out of plane and  $686\text{ cm}^{-1}$  is attributed to zerovalent iron,  $\text{Fe}^0$  as reported in the literature [28, 29, 30].

### **Optimization of pH, Contact time and Initial Concentration.**

Effect of pH places one of the greatest roles in the adsorption studies because it influences the surface charge of the adsorbents, ionic mobility, the degree of ionization and speciation of different pollutants and solution chemistry of contaminants (i.e. hydrolysis, redox reactions, polymerization and coordination) [26]. Fig 3 shows the plot the effect of pH on the sorption of  $\text{Cu}^{2+}$  onto nZVI. The percentage removal efficiency increases greatly from pH 4 (68.158 %) to pH 6 (86.3 %) where it attained equilibrium. The low percentage removal efficiency observed from pH 1 to 3 is a result of increase in electrostatic effect arising from the competition among  $\text{Cu}^{2+}$ ,  $\text{H}_3\text{O}^+$  and

other cationic species ( $\text{Cu}(\text{OH})^+$ ,  $\text{Cu}(\text{OH})_2$ ,  $\text{Cu}(\text{OH})_3^-$  and  $\text{Cu}(\text{OH})_4^{2-}$ ) for adsorption sites at lower pH. As the pH of the solution increases, the competition for adsorption site reduces and more of  $\text{Cu}^{2+}$  dominates thereby leading to increase in the quantity adsorbed (34.08 mg/g – 43.15 mg/g) and considerable increase in the percentage removal efficiency. The optimum pH observed was pH 6 and all other optimization studies were carried out at this pH [12, 13, 14, 26].

The effect of adsorbent dose on the sorption of  $\text{Cu}^{2+}$  onto nZVI is shown on Fig 4. Increase in the adsorbent dose from 18.99 mg/g at 10mg to 22.62 mg/g was a result of increase in the number of active site as the adsorbent increases. This is similar to findings reported in the literature [30].

The effect of contact time (Fig 5) is another important factor in all transfer phenomena such as adsorption. A short contact time to reach equilibrium indicates the fast transport of  $\text{Cu}^{2+}$  ions from the bulk to the outer and inner surface of nZVMn. In addition, contact time also controls the buildup of charges at the solid-liquid interfaces and for this reason, optimization of the contact time on the effect of sorption of  $\text{Cu}^{2+}$  onto nZVI was investigated at three different initial concentrations 40ppm, 60ppm and 100ppm from 10min to 120min. The rate of reaction was rapid from 10 min with 16.878 mg/g, 25.854 mg/g and 40.03 mg/g

(Fig 5) at the three concentrations respectively. The contact time of 60 minutes was observed as the optimum time after which a steady state approximation set in and a quasi-equilibrium situation was attained. All other optimization studies were carried out at 60 minutes contact time. Fig. 6 shows the result of the effect of initial  $\text{Cu}^{2+}$  ion concentration on the sorption of  $\text{Cu}^{2+}$  onto nZVI. As the initial concentration increased from 10ppm to 100ppm, the percentage removal efficiency also increased as a result of available and vacant active sites at low concentration and as the concentration increased, the active site became saturated and a state of equilibrium was attained where there was no significant increase in the percentage removal efficiency [25, 31]

### Adsorption Kinetics

The kinetic models were exploited to test the experimental data obtained from contact times ranging from 10 to 120 minutes by monitoring the quantity of  $\text{Cu}^{2+}$  adsorbed. In order to determine the mechanisms of sorption and its potential rate controlling steps which include mass transport and chemical reaction process, pseudo first-order, pseudo second-order, Elovich, power function (fractional power) and intraparticle diffusion rate equations have been used to model the kinetics of sorption of  $\text{Cu}^{2+}$  onto nZVI. The constant parameters, correlation coefficient ( $R^2$ ) and their values are summarized on Table 3

The pseudo first-order equation (Lagergren's equation) describes adsorption in solid-liquid systems based on the sorption capacity of solids. It is assumed that one copper ion was sorbed onto one sorption site on the nZVI surface [32]:



Where S represents an unoccupied sorption site on the nZVI  
The pseudo first-order equation is generally expressed as:

$$\frac{dq}{dt} = k_1(q_e - q_t) \quad (5)$$

where  $q_e$  is the amount of  $\text{Cu}^{2+}$  adsorbed at equilibrium per unit weight of the adsorbent (mg/g),  $q_t$  is the amount of  $\text{Cu}^{2+}$  adsorbed at any time (mg/g) and  $k_1$  is the pseudo first-order rate (constant/min). After the equation is integrated and boundary conditions ( $t = 0 \rightarrow t$  and  $q_t = 0 \rightarrow q_t$ ) are applied the equation becomes:

$$\text{Log}(q_e - q_t) = \text{Log } q_e - \frac{k_1 t}{2.303} \quad (6)$$

The values of  $\text{Log}(q_e - q_t)$  were linearly correlated with  $t$ . The plot of  $\text{Log}(q_e - q_t)$  versus  $t$  as shown on Fig. 7 gave a linear relationship and  $k_1$  and  $q_e$  were determined from the slope and intercept of the expression in Eq. 5 respectively. The parameters are summarized on Table 3 and it showed that the kinetics model did not fit into pseudo first order model equation because the correlation

coefficient was very low and the adsorption capacity calculated using this model was not close to the experimental quantity adsorbed indicating that the data were poorly fitted into pseudo first order (Hao et al., 2010)

The pseudo second-order rate expression, which has been applied for analyzing Chemisorption kinetics from liquid solutions [31, 32].

$$\frac{dq}{dt} = k_2(q_e - q_t)^2 \quad (7).$$

where  $k_2$  is the rate constant of for pseudo second-order adsorption equation (g/mg min). For the boundary conditions (  $t = 0 \rightarrow t$  and  $q_t = 0 \rightarrow q_t$ ), the integrated form of Eq. (6) is linearly expressed as:

$$\frac{t}{q_t} = \frac{1}{k_2 q_e^2} + \frac{1}{q_e} t \quad (8)$$

$$h_0 = k_2 q_e^2 \quad (9)$$

Substituting  $h_0$  into equation above, it becomes:

$$\frac{t}{q_t} = \frac{1}{h_0} + \frac{1}{q_e} t \quad (10)$$

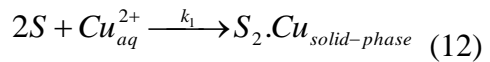
where  $h_0$  is the initial adsorption rate. The plot of  $t/q_t$  against  $t$  as shown on Fig. 8 gave a linear plot with good and commendable correlation coefficients close to unity at each concentration as shown on Table 3. The pseudo second-order parameters,

$k_2$ ,  $q_e$  and  $h_0$  were determined from the slope and intercept of Eq. 10

When  $t$  tends to 0,  $h_0$  is defined as:

$$h_0 = k_2 q_e^2 \quad (11)$$

This model assumes that one copper ion is sorbed onto two sorption sites on the nZVI surface:



From the parameters summarized on Table 3, the adsorption kinetics can be best described by pseudo second-order model. The  $R^2$  values at each concentration are greater than 0.99 and the calculated quantity adsorbed was perfectly close to experimental quantity adsorbed. This is in accordance with the findings reported in the literature [18, 32, 33, 34]

**The Elovich model** is generally described as:

$$\frac{dq}{dt} = \alpha \exp(-\beta q_t) \quad (13)$$

Applying the boundary conditions ( $q_t=0$  at  $t = 0$  and  $q_t = q_t$  at  $t = t$ ), the simplified form of the Elovich equation is expressed as [35]:

$$q_t = \frac{1}{\beta} \ln\left(\frac{\alpha}{\beta}\right) + \frac{1}{\beta} \ln(t) \quad (14)$$

where  $q_t$  is the amount of adsorbate per unit mass of sorbent at time ( $t$ ). The initial adsorption rate,  $\alpha$  (mg/g-min) and the desorption constant ( $\beta$ )

(g/mg) during any experiment were determined from the slope( $1/\beta$ ) and intercept  $(1/\beta)\ln(\alpha/\beta)$  of linear plot of  $q_t$  versus  $(t)$  as shown on Fig. 9. From the parameters on Table 3, it can be deduced that since the values of  $R^2$  were to unity and the adsorption rates were also high, the data could also be described by the Elovich model.

The Fractional power model can be expressed as [20,31]:

$$q_t = kt^v \quad (15)$$

The equation above is linearized as:

$$\log(q_t) = \log(k) + v \log(t) \quad (16)$$

where  $q_t$  is the amount of sorbate per unit mass of sorbent,  $k$  is the fractional power rate constant,  $t$  is time, and  $v$  is a positive constant ( $<1$ ). The parameters  $v$  and  $k$  were determined from slope and intercept of a linear plot of  $\log(q_t)$  versus  $\log(t)$  as shown on Fig. 10. The parameters shown on Table 3 indicated that the parameter fit also into the fractional model because the values of  $v$  were less than 1 and the regression coefficient ( $R^2$ ) was greater than 0.96 at optimum concentration [30]

The intraparticle diffusion equation as expressed by Weber-Morris is given as [35]:

$$q_t = k_{id}t^{0.5} + C \quad (17)$$

Where  $k_1$  is the intraparticle diffusion rate constant ( $\text{mg g}^{-1} \text{min}^{1/2}$ ) and  $C$  is the intercept determined from the linear plot of  $q_t$  versus  $t^{0.5}$  (Fig. 11). The intercept of the plot reflects the boundary layer effect. Higher values of the boundary layer effect obtained (16.246, 25.628 and 39.667) are indication greater contribution of the surface sorption in the rate controlling step. The calculated intraparticle diffusion coefficient ( $k_{id}$ ) values are listed in Table 3. Since the linear plot of  $q_t$  versus  $t^{1/2}$  did not pass through the origin, then intraparticle diffusion not the sole rate-limiting step [36].

### Adsorption Isotherms

The adsorption isotherm constant parameters, correlation coefficient ( $R^2$ ) and their values are summarized in Table 4.

Langmuir Adsorption Isotherm assumes a monolayer adsorption onto a homogeneous surface with a finite number of identical sites also there is uniform energy of adsorption onto the surface and no transmigration of adsorbate in the plane of the surface [37, 38]. The linear form of Langmuir represents:

$$\frac{C_e}{Q_e} = \frac{1}{K_L Q_{\max}} + \frac{C_e}{Q_{\max}} \quad (18)$$

$Q_{\max}$  is the maximum monolayer coverage capacity ( $\text{mg.g}^{-1}$ ),  $K_L$  is the Langmuir isotherm constant ( $\text{L.mg}^{-1}$ ) related to the energy of adsorption. The essential features of the

Langmuir isotherm may be expressed in terms of equilibrium parameter  $R_L$ , which is a dimensionless constant referred to as separation factor or equilibrium parameter [38].

$$R_L = \frac{1}{1 + K_L C_o} \quad (19)$$

Figure 12 shows the Langmuir isotherm model plot for sorption of  $\text{Cu}^{2+}$  onto nZVI. The Langmuir constants,  $Q_{\max}$  and  $K_L$  were determined from the linear plot of  $C_e/Q_e$  versus  $C_e$  as shown on Fig 12. The value of separation factor,  $R_L$  (Fig 13) indicates the adsorption nature to either unfavourable or unfavourable. If  $R_L > 1$ , it is unfavorable, linear if  $R_L = 1$ , favorable if  $0 < R_L < 1$  and irreversible if  $R_L = 0$ . Since the value of separation factor ( $R_L$ ) ranges from 0.110 at 10ppm to 0.021 at 100ppm and none of them was greater than 1 therefore, the adsorption of  $\text{Cu}^{2+}$  onto nZVI was favourable. In addition, the regression coefficient ( $R^2 > 0.90$ ) and maximum monolayer coverage capacity ( $Q_{\max} = 40.816 \text{ mg/g}$ ) revealed that the equilibrium sorption can be best described by Langmuir model which supported a chemisorption mechanism

The Freundlich sorption isotherm gives an expression encompassing the surface heterogeneity and the exponential distribution of active sites

and their energies. The Linear form of Freundlich equation is [36, 37]:

$$\log Q_e = \log K_f + \frac{1}{n} \log C_e \quad (20)$$

The Freundlich isotherm constants,  $K_f$  and  $n$  are parameters characteristic of the sorbent-sorbate system, which were determined from the intercept and slope of the plot of  $\text{Log}Q_e$  against  $\text{Log}C_e$  (Fig 14) from the Table 4, the value of  $n$  (2.853) less than 10 is also an indication of a favourable adsorption. However, the sorption data could not be best described by Freundlich model compared to Langmuir model.

Temkin Isotherm contains a factor that explicitly taking into the account of adsorbent–adsorbate interactions in a chemisorption mechanism. The model assumes that heat of adsorption (function of temperature) of all molecules in the layer would decrease linearly with the surface coverage due to adsorbent–adsorbate interactions. The linear form of the equation is given as [39]:

$$Q_e = \frac{RT}{b_T} \ln A_T + \frac{RT}{b_T} \ln C_e \quad (21)$$

Where  $B = RT/b_T$ ,  $b_T$  is the Temkin isotherm constant related to the heat of sorption and  $A_T$  is the Temkin isotherm equilibrium binding constant ( $\text{Lg}^{-1}$ ). The values of these constants were determined from the slope and intercept obtained from appropriate plot of  $Q_e$  versus  $\ln C_e$  as shown in figure 15 and are clearly shown on

Table 4. The high value of coefficient of regression ( $R^2 = 0.937$ ) obtained from Temkin model corroborated the chemisorption mechanism as inferred from Langmuir Model.

**Dubinín–Kaganer–Radushkevich (DKR) isotherm model** is generally applied to express the adsorption mechanism with a Gaussian energy distribution onto a heterogeneous surface. The model has often successfully fitted high solute activities and the intermediate range of concentrations data well. The linear equation is given by [36, 37, 38, 39]:

$$\ln Q_e = \ln Q_d - A_{D-R} \varepsilon^2 \quad (22)$$

Where  $A_{D-R}$  is the DRK isotherm constant ( $\text{mol}^2/\text{kJ}^2$ ) related to free sorption energy and  $Q_d$  is the theoretical isotherm saturation capacity ( $\text{mg/g}$ ). The values of  $A_{D-R}$  and  $Q_d$  were determined respectively from the slope and intercept of the plot of  $\ln Q_e$  versus  $\varepsilon^2$  (Fig 16). The parameter  $\varepsilon$  is the Polanyi potential which is computed as:

$$\varepsilon = RT \ln \left[ 1 + \frac{1}{C_e} \right] \quad (23)$$

The approach was usually applied to distinguish the physical and chemical adsorption of metal ions with its mean sorption free energy,  $E$  per molecule of adsorbate (for removing a molecule from its location in the sorption space to the infinity) can be computed by the relationship [40]:

$$E = - \left[ \frac{1}{\sqrt{2A_{D-R}}} \right] \quad (24)$$

If the value of mean sorption free energy ( $E$ ) is less than  $8\text{kJ mol}^{-1}$ , the adsorption mechanism will be physisorption and if the value of  $E$  is greater than  $8\text{kJ mol}^{-1}$ , the adsorption will be chemisorption. Since the magnitude of  $E$  (free energy of transfer of one solute from infinity to the surface of nZVI) is greater than  $8\text{KJ mol}^{-1}$  (Table 4), the adsorption mechanism is chemisorption which further supported Langmuir Isotherm [39].

Both Halsey isotherm and Harkin-Jura are used to evaluate the multilayer adsorption at a relatively large distance from the surface. The Halsey isotherm is expressed by [36, 39]:

$$\ln q_e = \left[ \left( \frac{1}{n_H} \right) \ln K \right] - \left( \frac{1}{n_H} \right) \ln C_e \quad (25)$$

A plot of  $\ln q_e$  against  $\ln C_e$  gave a linear graph (Fig 17) and the Halsey constants  $K_H$  and  $n_H$  were determined from the intercepts and slope respectively. The Halsey isotherm model is always in support of Freundlich model and an evidence of this is shown from the regression coefficient ( $R^2 = 0.874$ ) which is similar to that obtained from Freundlich model. Both Freundlich and Halsey models always support

multilayer adsorption [39]. A low regression coefficient obtained from both Freundlich and Hasley models is an indication that the equilibrium data did not follow multilayer adsorption.

The Harkin-Jura isotherm is expressed as:

$$\frac{1}{q_e^2} = \frac{B_{HJ}}{A_{HJ}} - \frac{1}{A_{HJ}} \log Ce \quad (26)$$

The Harkin-Jura constants  $A_{HJ}$  and  $B_{HJ}$  were determined from the slope and intercept of the linear plot of  $\frac{1}{q_e^2}$  versus  $\log Ce$  as shown on figure 18. The parameters of Harkin-Jura isotherm model are as shown on Table 4 revealed that the equilibrium sorption data is poorly described by this model which further supported chemisorption process.

### Thermodynamics studies

Temperature is another important parameter in the adsorption studies because some important parameters like enthalpy change ( $\Delta H$ ), entropy change ( $\Delta S$ ) and Gibbs free energy change ( $\Delta G$ ) could be determined. The thermodynamic parameters can be determined from the thermodynamic equilibrium constant,  $K_a$  (or the thermodynamic distribution coefficient). The standard Gibbs free energy  $\Delta G^\circ$  ( $\text{kJ mol}^{-1}$ ), standard enthalpy change  $\Delta H^\circ$  ( $\text{kJ mol}^{-1}$ ), and standard entropy change  $\Delta S^\circ$  ( $\text{J mol}^{-1}\text{K}^{-1}$ ) were calculated using the following equations [30, 40]:

$$Ka = \frac{q_e}{Ce} \quad (27)$$

$$\Delta G = -RT \ln Ka \quad (28)$$

$$\text{Log}Ka = \frac{\Delta S}{2.303R} - \frac{\Delta H}{2.303RT} \quad (29)$$

The Van't Hoff plot on sorption of  $\text{Cu}^{2+}$  onto nZVI is shown on Fig. 19 and the thermodynamics parameters are stated on Table 5. The positive standard enthalpy change ( $\Delta H^\circ = 53.44925 \text{ kJmol}^{-1}$ ) for this study suggests that the adsorption of  $\text{Cu}^{2+}$  by nZVI is endothermic in nature, which is supported by the increase in  $\text{Cu}^{2+}$  adsorption with increase in temperature from 298 K to 318 K. The positive standard entropy change ( $\Delta S^\circ = 45.3 \text{ Jmol}^{-1} \text{ K}^{-1}$ ) reflected the affinity of the nZVI particles towards  $\text{Cu}^{2+}$  and the negative values of the standard Gibbs free energy  $\Delta G^\circ$  (Table 5) is an indication of the feasibility and spontaneity of the adsorption process.

### Conclusion

The synthesis of nanoscaled zerovalent iron via single pot system vis-à-vis chemical reduction is a novel approach. The isotherms, kinetics and thermodynamics studies of sorption of  $\text{Cu}^{2+}$  onto zerovalent iron nanoparticles was investigated. Optimization studies revealed that pH, contact time, initial concentration, adsorbent dose and temperature played substantial role in

adsorption studies and maximum adsorption capacity can be obtained at pH 6 for sorption of  $\text{Cu}^{2+}$ . The pseudo first-order, pseudo second-order, Elovich, power function (fractional power) and intraparticle diffusion rate equations have been used to model the kinetics of sorption of  $\text{Cu}^{2+}$  and from this investigation, pseudo second-order best described the kinetic process. From the six different adsorption isotherm models investigated, equilibrium sorption data fitted best into Langmuir and Temkin isotherm models indicating a Chemisorption mechanism and this was also supported with the high energy value calculated from DRK isotherm model which is in the range of the energy values for

Chemisorption process. The values obtained from the thermodynamics parameters,  $\Delta H$ ,  $\Delta S$ , and  $\Delta G$  vividly proved the reaction was feasible, spontaneous and endothermic in nature. Outcome of this research showed that zerovalent iron nanoparticle is an effective and promising nano-adsorbent for the sorption of toxic heavy metal ions.

### Acknowledgement

Dada, Adewumi Oluwasogo wishes to appreciate the management of Landmark University for providing enabling environment and facilities for novel, result oriented research and opportunity to carry out my Ph.D. programme in University of Ilorin.

### References

- Brewer, G.J. (2010). Copper toxicity in the general population. *Clin Neurophysiol.* 121(4):459-60. doi:10.1016/j.clinph.2009.12.015 PMID 20071223
- Casarett and Doull's Toxicology, The Basic Science of Poisons, Fifth Edition, Edited by Curtis D. Klassen, Ph.D., McGraw-Hill, New York. pp 715.
- Kardiravela, K and Namsasivayan, C. (2003). "Activated carbon from coconut coir- pith as metal adsorbent: adsorption of Cd (II) aqueous solution" . *Advances in Environmental Researcher* 411 – 418.
- Richard, A.L and Tay O.C (1980) *Encyclopedia Americana*, pp 137 – 139.
- Yoon, Y., Amy, G. and Yoon, J. (2005). "Effect of pH and conductivity on hindered diffusion of per chlorate ions during transport through negatively charged nanofiltration and ultra-filtration membranes". *Desalination* 177: 217-227
- Crittenden, J., Trusell, R., Hand, D., Howe, K., and Techobanoglous, G. (2005). *Water treatment principle and design*, 2<sup>nd</sup> Edition John Wiley & Sons. New Jersey.

- Ku, Y., Wu, M-H., and Shen Y-S., (2002). "A study on the cadmium removal from aqueous solutions by zinc cementation". *Separation Science and Technol.*, 37 (3): 571-590.
- Singh, K. K., Talat, M., and Hasan, S. H., (2006) Removal of lead from aqueous solutions by agricultural waste maize bran". *Bioresource Technol.*, 97 (16): 2124-2130
- Elizabeth de Olivera, Maria, J. and Santos, Y. (2003), 'Heavy metals removal in industrial Effluent by sequential adsorbent treatment', *Advancement in Environmental Research*. 7(2): 263 – 272.
- Kamimura, Y., Chiba, H., and Utsumi, H (2002). "Barrier function of micro vessels and roles of glial cell line-derived neurotrophic factor in the rat testis," *Medical Electron Microscopy*, Vol.35, pp. 139–145.
- Jovanovic, M., Rajic, N., and Obradovic, B. (2012). Novel kinetic model of the removal of divalent heavy metal ions from aqueous solutions by natural clinoptilolite, *Journal of Hazardous Materials* 233–234: 57– 64
- Hao Y-M., Chen, M., Hu, Z-B (2010). Effective removal of Cu (II) ions from aqueous solution by amino-functionalized magnetic nanoparticles, *Journal of Hazardous Materials* 184: 392–399
- Gong, J-L., Wang, X-Y., Zeng, G-M., Chen, L., Deng, J-H., Zhang, X-R., Ni, Q-Y. (2012). Copper (II) removal by pectin–iron oxide magnetic nanocomposite adsorbent. *Chemical Engineering Journal* 185–186: 100 – 107
- Badruddoza, A.Z.M., Tay, A.S.H., Tan, P.Y., Hidajat, K., Uddin, M.S (2011) Carboxymethyl- cyclodextrin conjugated magnetic nanoparticles as nano-adsorbents for removal of copper ions: Synthesis and adsorption studies, *Journal of Hazardous Materials* 185: 1177–1186
- Xiao, S., Ma, H., Shen, M., Wang, S., Huang, Q., Shi, X. (2011). Excellent copper (II) removal using zerovalent iron nanoparticle-immobilized hybrid electrospun polymer nano-fibrous materials, *Colloids and Surfaces A: Physicochemical. Eng. Aspects* 381: 48–54
- Liu, W., Ting Wang, T., Borthwick, A.G.L., Wang, Y., Yin, X., Li, X., Ni, J. (2013) Adsorption of  $Pb^{2+}$ ,  $Cd^{2+}$ ,  $Cu^{2+}$  and  $Cr^{3+}$  onto titanate nanotubes: Competition and effect of inorganic ions. *Science of the Total Environment* 456–457: 171–180
- Onundi, Y.B., Mamun, A.A., Al Khatib, M.F. and Ahmed, Y.M

- (2010). Adsorption of copper, nickel and lead ions from synthetic semiconductor industrial wastewater by palm shell activated carbon *International Journal of Environ. Sci. Tech.*, **7**(4): 751-758.
- Boparai, H.K., Meera, J., Dennis, M.O. (2010) Kinetics and thermodynamics of Cadmium ion removal by adsorption onto nano zerovalent iron particles. *Journal of Hazard. Mater.*, *Doi:10.1016/j.jhazmat.2010.11.029*
- Dada, A.O., Adekola, F.A and Odebunmi, E.O (2014). Investigation of the Synthesis and Characterization of Manganese Nanoparticles and its Ash Rice Husk Supported Nanocomposite, *Book of Proceedings of 1<sup>st</sup> African International Conference/Workshop on Applications of Nanotechnology to Energy, Health and Environment – March 23<sup>rd</sup> – 29<sup>th</sup>, 2014.* pg 62.
- Adekola, F.A., Abdu's Salam, N., Adegoke, H.I., Adekola, A.M., and Adekeye, J.I.D (2012) Removal of Pb (II) from aqueous solution by natural and synthetic calcites. *Bulletin Chemical Soc. Ethiop.* **26** (2): 195-210.
- Dada, A.O., Ojediran, J.O., and Olalekan, A.P., (2013). Sorption of Pb<sup>2+</sup> from Aqueous Solution unto Modified Rice Husk: Isotherms Studies. *Advances in Physical Chemistry*, <http://dx.doi.org/10.1155/2013/842425>
- Vasuderan, P., Padmavathy, V., Dhingra, S.C. (2003). “Kinetics of biosorption of Cadmium on Baker's yeast”. *Bioresources. Technology.* **89**(3):28-287
- Xu, H., Liu, Y., Tay, J. (2006). “Effect of pH on nickel biosorption by aerobic granular sludge”. *Bioresources Technology.* **97**(3): 359-363.
- Igwe, J.C., Abia, A.A., Ibeh, C.A., 2005. Adsorption kinetics and intraparticulate diffusivities of Hg, As and Pb ions on unmodified and thiolated coconut fiber. *International Journal of Environ. Sci. Technol.* **5**: 83–92 .
- Srivastava, V. C., Mall, I. D., Mishra, I.M. (2005). “Characterization of mesoporous rice husk ash (RHA) and adsorption kinetics of metal ions from aqueous solution onto RHA”. *Journal of hazardous material*, *doi:10.1016/j.jhazmat.11.052*.
- Chen, L., Sun, L.J., Luan, F., Liang, Y., Li, Y., Liu, X.X. (2010). Synthesis and pseudo capacitive studies of composite films of polyaniline and manganese oxide nanoparticles. *Journal of Power Sources*, **195**: 3742–3747
- Shahwan, T., Sirriah, A.S.; Nairat, M.; Boyacı, E.; Eroglu, A.E.;

- Scott, T.B.; Hallam. K.R. (2011). Green synthesis of iron nanoparticles and their application as a Fenton-like catalyst for the degradation of aqueous cationic and anionic dyes, *Chemical Engineering Journal*, 172: 258– 266
- Prema, P., Thangapandian, S., Selvarani, M., Subharanjani, S., C. Amutha (2011) Color removal efficiency of dyes using nano zerovalent iron treatment. *Toxicological & Environmental Chemistry*, 93:10, 1908-1917
- Frost, R.L., Xi, Y., He, H. (2010). Synthesis, characterization of palygorskite supported zerovalent iron and its application for methylene blue adsorption, *Journal of Colloid and Interface Science* 341: 153–161
- Ayanda, O.S., Fatoki, S.O., Adekola, F.A and Ximba, B.J. (2013) Kinetics and equilibrium models of the sorption of tributyltin to nZnO, activated carbon and nZnO/activated carbon composite in artificial seawater. *Marine Pollution Bulletin.*, <http://dx.doi.org/10.1016/j.marpolbul.2013.04.001>
- Ho, Y.S. (2004) Citation review of Lagergren kinetic rate equation on adsorption reactions, *Scientometrics*, 59:171–177.
- Ho, Y.S. (2006) Review of second-order models for adsorption systems, *Journal of Hazardous Material*. 136: 681–689.
- Azizian, S. (2004) Kinetic models of sorption: a theoretical analysis, *Journal of Colloid Interface Sci.* 276: 47–52.
- Hameed, B.H, D.K. Mahmoud, D.K. A.L. Ahmad, A.L. (2008) Equilibrium modeling and kinetic studies on the adsorption of basic dye by a low-cost adsorbent: Coconut (*Cocos nucifera*) bunch waste, *Journal of Hazardous Materials* 158: 65–72
- Igwe, J. C. and Abia A.A. (2006) A bioseparation process for removing heavy metals from waste water using biosorbents, *African Journal of Biotechnology* 5 (12), pp. 1167-1179
- Bhatt, R.R., Shah, B.A. (2013). Sorption studies of heavy metal ions by salicylic acid–formaldehyde–catechol terpoly-meric resin: Isotherm, kinetic and thermodynamic cs. *Arabian Journal of Chemistry*, <http://dx.doi.org/10.1016/j.arabjc.2013.03.012>
- Foo, K.Y and Hameed, B.H (2010) Insights into the modeling of adsorption isotherm systems. *Chemical Engineering Journal*, 156: 2–10
- Argun, M.E., Dursun, S., Ozdemir, C. and Karatas, M. (2007) Heavy metal adsorption by modified oak sawdust: Thermodynamics and kinetics.

*Journal of Hazardous Materials*, 141: 77–85

Chengwen, S., Shuaihua, W., Murong, C., Tao, P., Mihua, S and Guangrui, G. (2014). Adsorption Studies of Coconut Shell Carbons Prepared by KOH Activation for Removal of Lead(II) From Aqueous Solutions *Sustainability*, **6**: 86-98; doi:10.3390/su6010086

Ahmad, M.A., Ahmad, N., and Bello, O.S (2014): Removal of Remazol Brilliant Blue Reactive Dye From Aqueous Solutions Using Watermelon Rinds as Adsorbent, *Journal of Dispersion Science and Technology*  
<http://dx.doi.org/10.1080/01932691.2014.925400>

### List of Figures and Tables

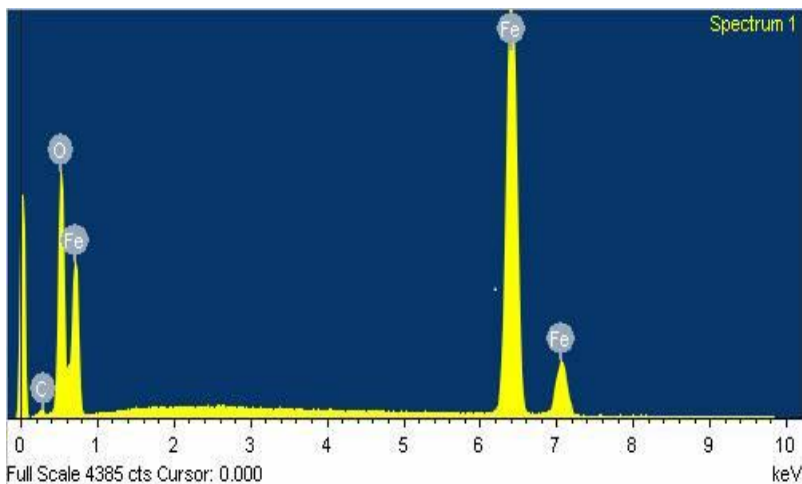
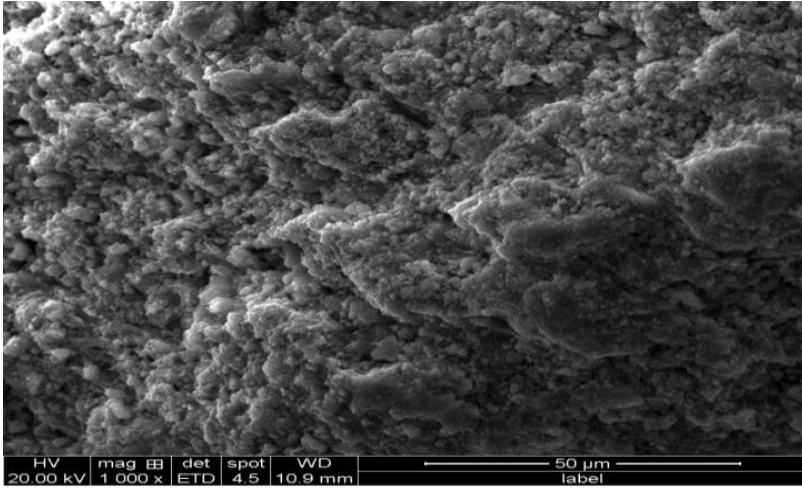


**Fig 1: EDX spectrum for nZVI**



**SEM micrograph for nZVI**

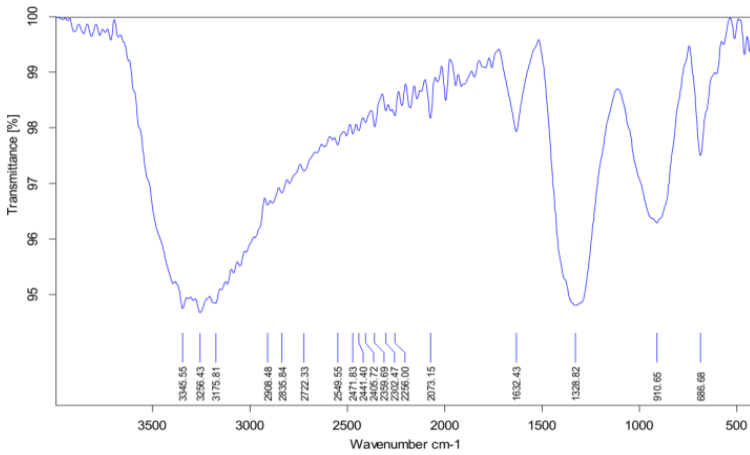


**Fig 2: FTIR spectrum for nZVI**

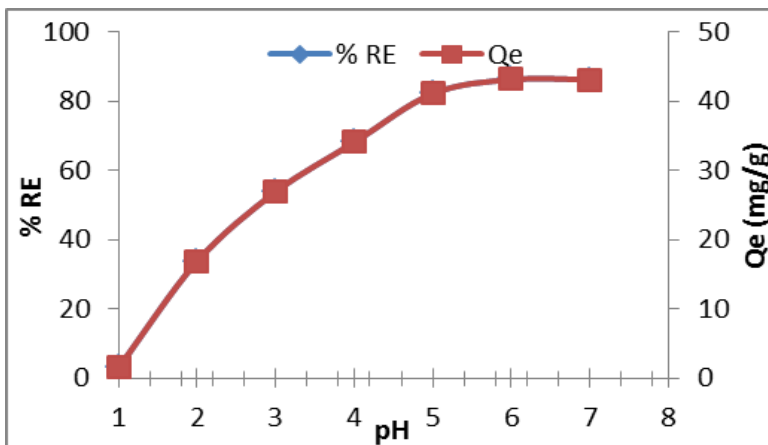


**Fig 3: Effect of pH on sorption of Cu<sup>2+</sup> onto nZVI**

Experimental conditions: Cu<sup>2+</sup> Concentration = 100 mg/L  
 Volume of Cu<sup>2+</sup> solution = 50 mL; Contact time = 60 min,  
 Stirring speed = 200 rpm, Adsorbent Dose = 100 mg  
 and Temperature = 25 ± 2 °C

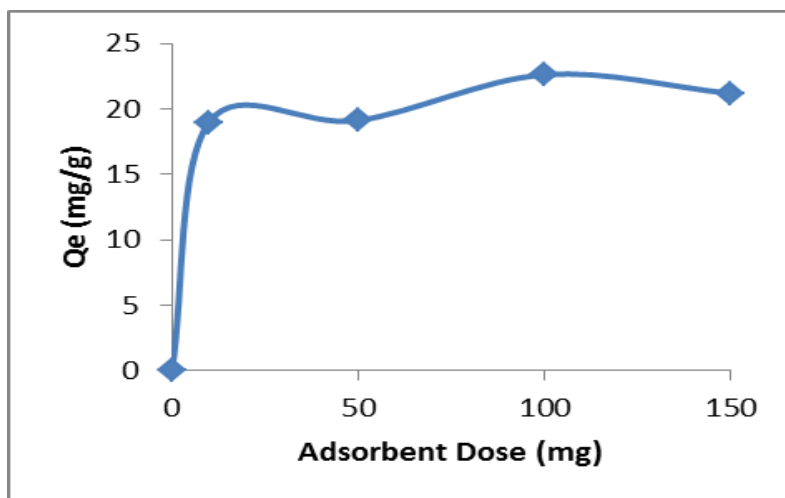


**Fig 4: Effect of Adsorbent dose on sorption of Cu<sup>2+</sup> onto nZVI**

Experimental conditions: Cu<sup>2+</sup> Concentration = 100 mg/L  
 Volume of Cu<sup>2+</sup> solution = 50 mL; pH = 6, stirring speed = 200 rpm,  
 Contact time = 60 min, and temperature = 25 ± 2 °C

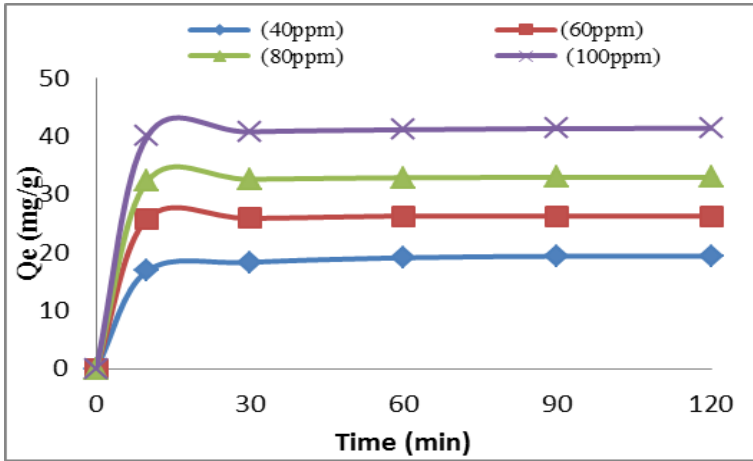


**Fig 5: Effect of Contact time on sorption of Cu<sup>2+</sup> onto nZVI**

*Experimental conditions: Cu<sup>2+</sup> Concentration= 100 mg/L  
 Volume of Cu<sup>2+</sup> solution = 50 mL; pH = 6, stirring speed = 200 rpm  
 Adsorbent Dose =100 mg and temperature = 25 ± 2 °C*

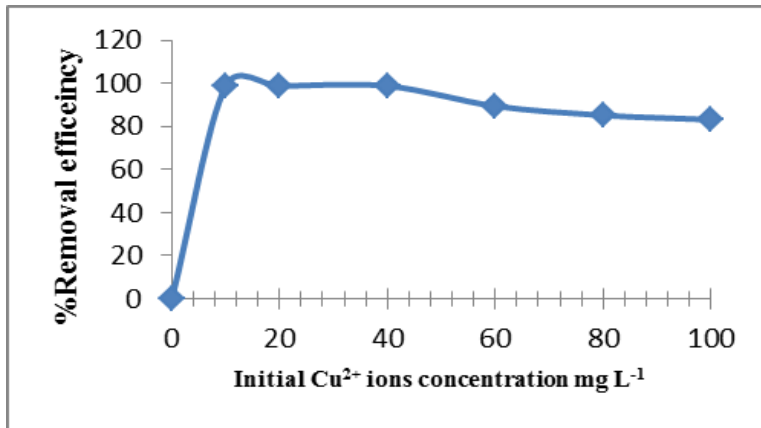


**Fig 6: Effect of Initial Concentrations**

*Experimental conditions: Volume of Cu<sup>2+</sup> solution = 50 mL;  
 Contact time = 60 min, pH = 6; Stirring speed = 200 rpm;  
 Adsorbent Dose =100 mg and Temperature = 25 ± 2 °C*

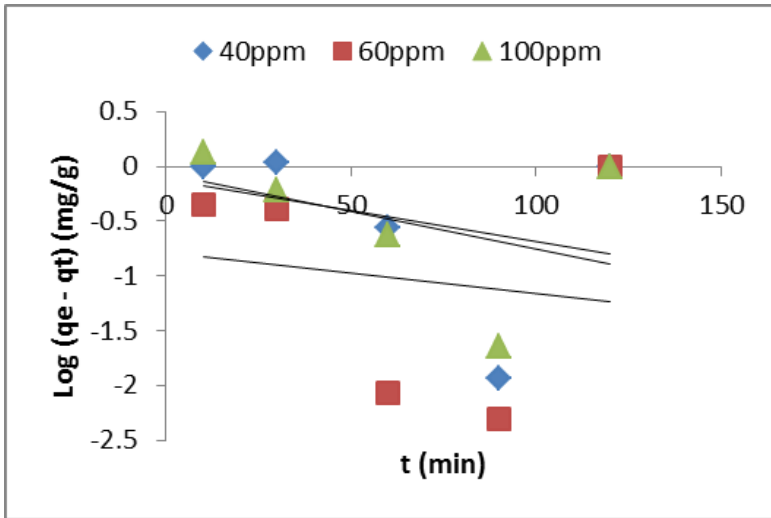


Fig 7: Pseudo first-order kinetic of sorption of  $\text{Cu}^{2+}$  onto nZVI

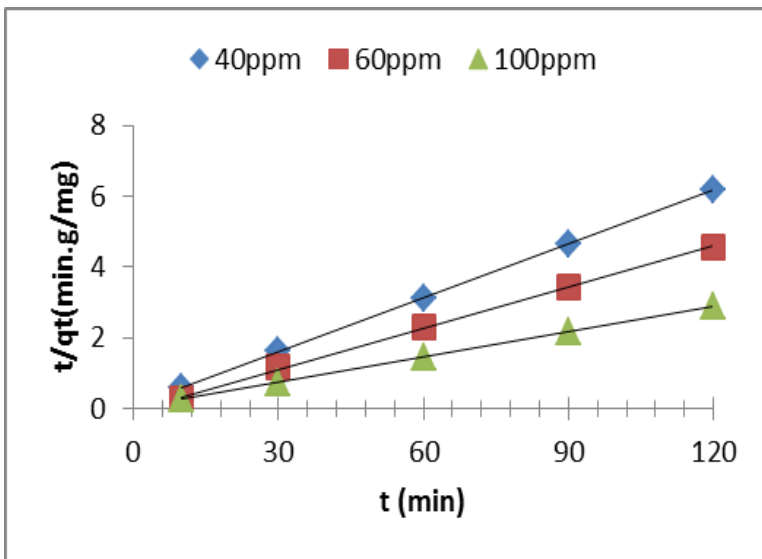
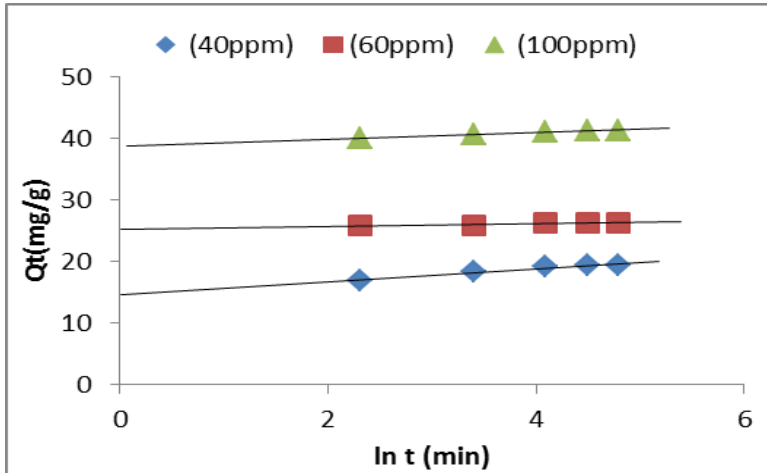
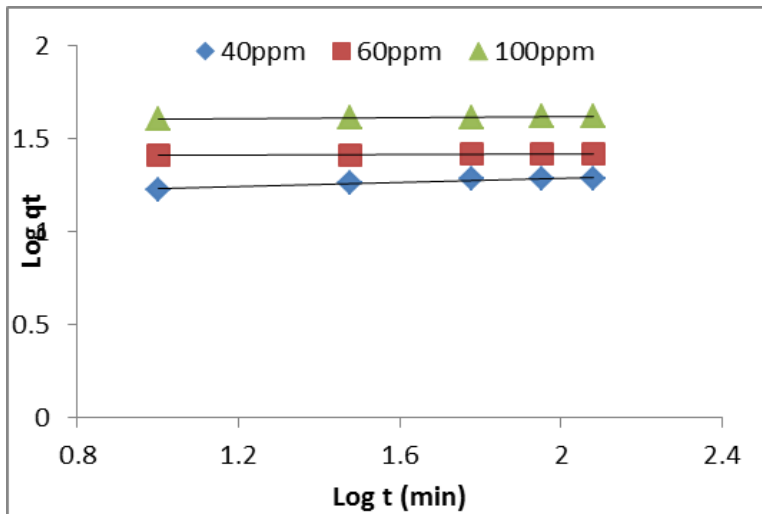


Fig 8: Pseudo second-order kinetic of sorption of  $\text{Cu}^{2+}$  onto nZVI



**Fig 9: Elovich model of sorption of  $\text{Cu}^{2+}$  onto nZVI**



**Fig 10: Fractional power of sorption of  $\text{Cu}^{2+}$  onto nZVI**

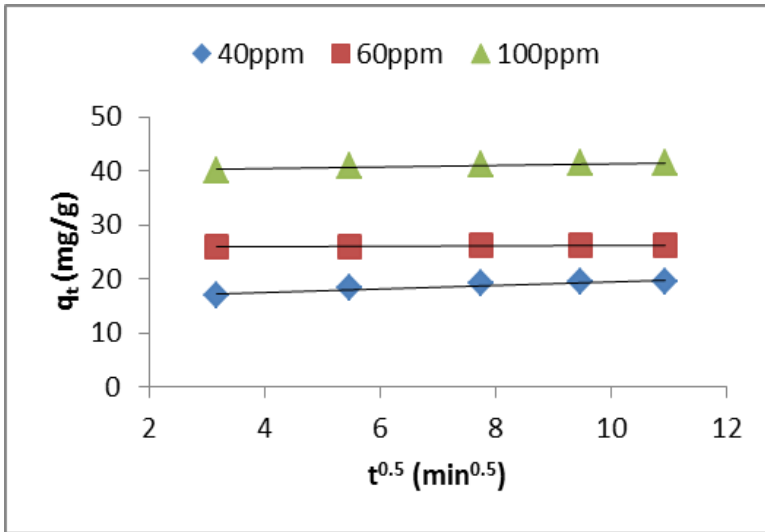


Fig 11: Intraparticle diffusion plot for sorption of  $\text{Cu}^{2+}$  onto nZVI

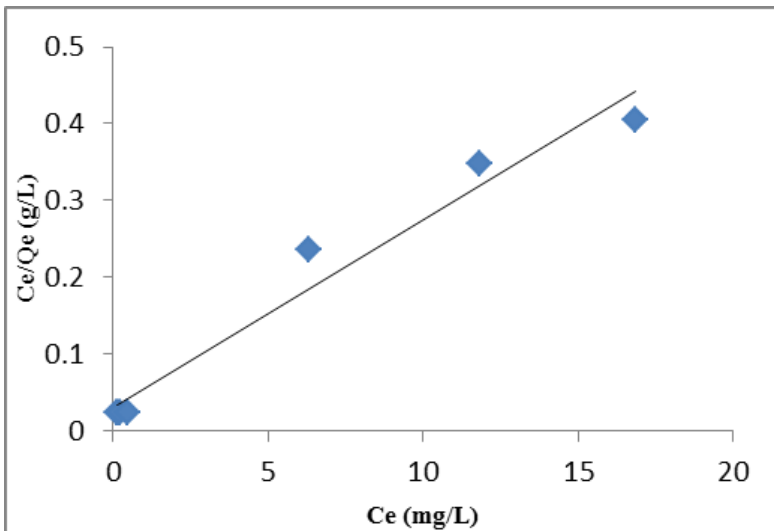


Fig 12: Langmuir Isotherm model for sorption of  $\text{Cu}^{2+}$  onto nZVI

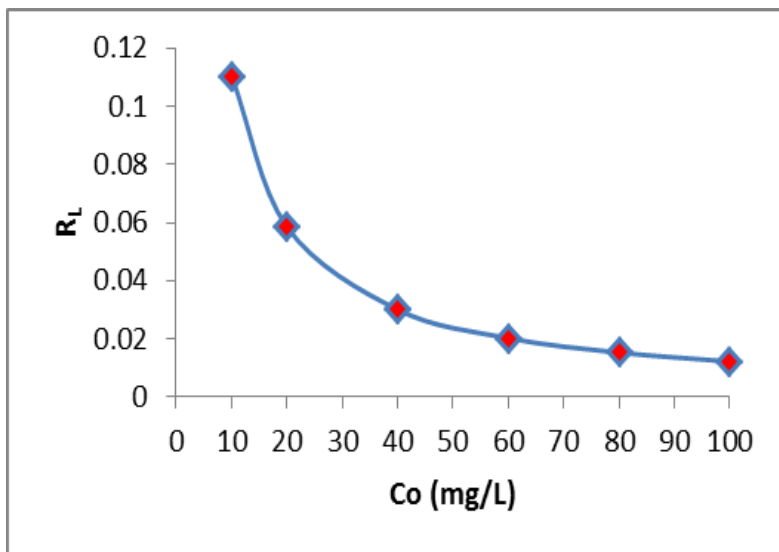


Fig 13: Separation factor on sorption of  $Cu^{2+}$  onto nZVI

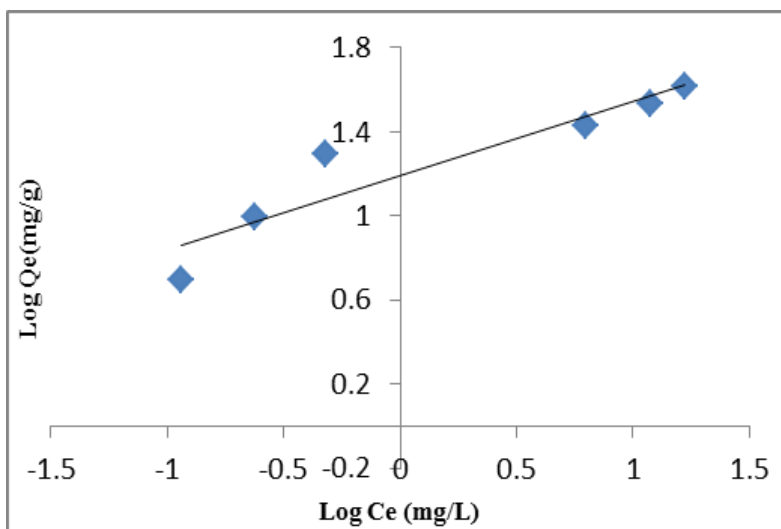


Fig 14: Freundlich Isotherm model for sorption of  $Cu^{2+}$  onto nZVI

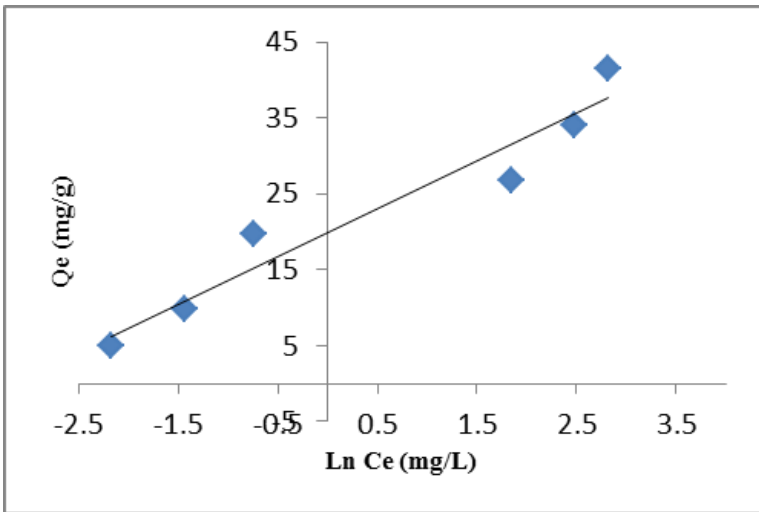


Fig 15: Temkin Isotherm model for sorption of  $\text{Cu}^{2+}$  onto nZVI

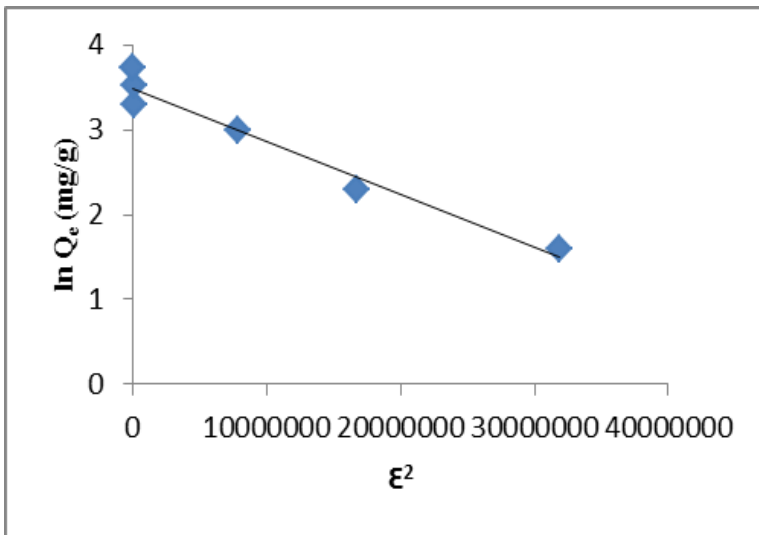


Fig 16: DRK Isotherm model for sorption of  $\text{Cu}^{2+}$  onto nZVI

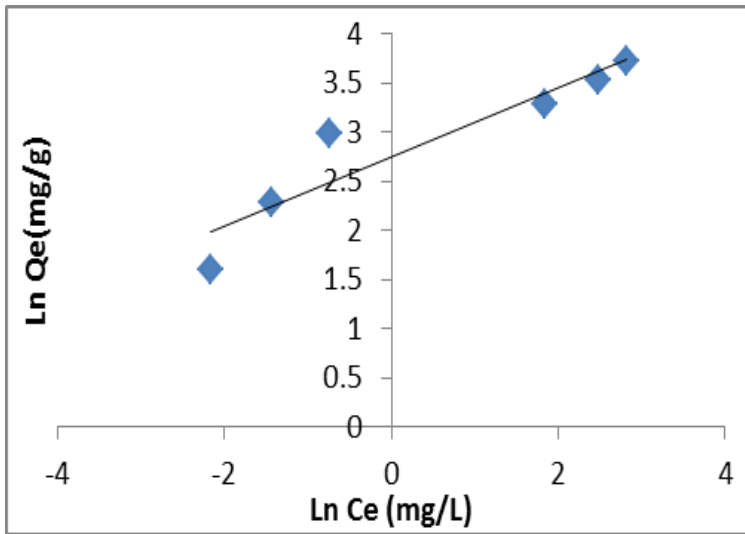


Fig 17: Halsey Isotherm model for sorption of  $\text{Cu}^{2+}$  onto nZVI

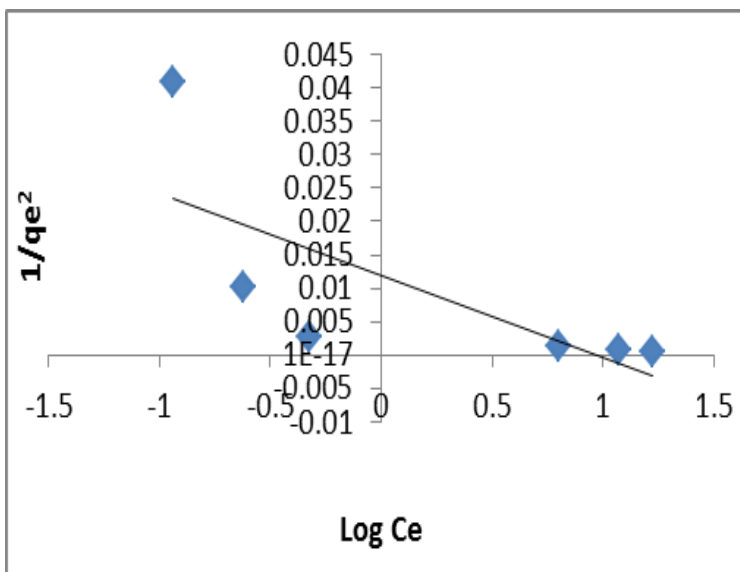


Fig 18: Harkins-Jura Isotherm model for sorption of  $\text{Cu}^{2+}$  onto nZVI

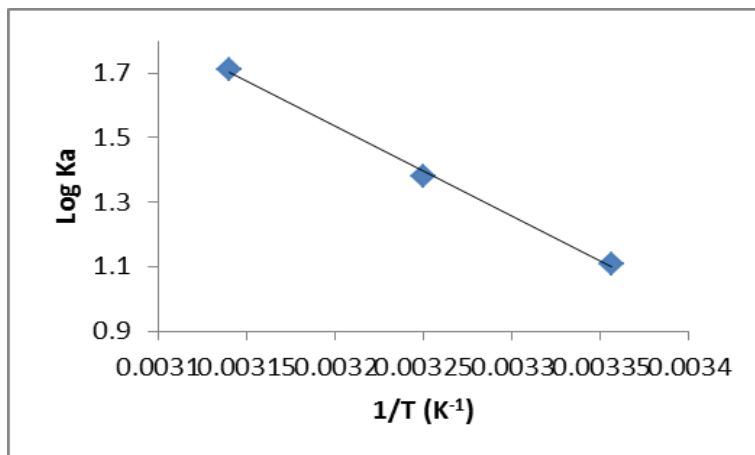


Fig 19: Van't Hoff plot on sorption of Cu<sup>2+</sup> onto nZVI

**Table 1: Physicochemical parameters of nZVI as adsorbent for the sorption of Cu<sup>2+</sup>**

pH	6.00
PZC	5.20
<b>BET Surface Area:</b>	20.8643 m <sup>2</sup> /g
t-Plot Micropore Area:	4.4140 m <sup>2</sup> /g
t-Plot External Surface Area:	16.4503 m <sup>2</sup> /g
BJH Adsorption cumulative surface area of pores between 17.000 Å and 3000.000 Å diameter:	19.120 m <sup>2</sup> /g
<b>Pore Volume</b>	
Single point adsorption total pore volume of pores less than 1070.322 Å diameter at P/P <sub>0</sub> = 0.981571614:	0.097502 cm <sup>3</sup> /g
t-Plot micropore volume:	0.001895 cm <sup>3</sup> /g
BJH Adsorption cumulative volume of pores between 17.000 Å and 3000.000 Å diameter:	0.115083 cm <sup>3</sup> /g
<b>Pore Size</b>	
Adsorption average pore width (4V/A by BET):	186.9268 Å
BJH Adsorption average pore diameter (4V/A):	240.753 Å

**Table 2: EDX Elemental percentage composition of NZVI**

Element	Weight%	Atomic%
C K	1.72	4.75
O K	21.24	43.97
Fe K	86.47	51.28
Totals	109.43	100

**Table 3: Kinetic model parameters for Cu<sup>2+</sup> adsorption onto nZVI investigated at different concentrations**

Models	40ppm	60ppm	.00ppm
pseudo first-order			
$k_1$	0.0159	0.00875	0.0131
$qe,exp$	19.388	26.305	41.39
$qe,cal$	0.855	0.163	0.763
$R^2$	0.131	0.0242	0.124
Pseudo second-order			
$k_2$	0.0264	0.1177	0.0538
$qe,exp$	19.388	26.305	41.39
$qe,cal$	19.723	25.773	41.49
$H_0$	10.256	13.928	92.593
$R^2$	1	0.999	1
Elovich			
$\alpha$	10.09x10 <sup>5</sup>	48.196	3.932
$\beta$	0.944	4.673	1.771
$R^2$	0.968	0.837	0.982
Fractional Power			
$K$	14.887	25.322	38.833
$V$	0.0583	0.0082	0.0139
$R^2$	0.963	0.837	0.981
Intra-particle Diffusion			
$K$	0.0322	0.0683	0.1735
$C$	16.246	25.628	39.667
$R^2$	0.881	0.835	0.909

**Table 4: Langmuir, Freundlich, Temkin, and D–R, Halsey and Harkin-Jura isotherm models parameters and correlation coefficients for adsorption of copper ions onto nZVI particles**

Isotherm Models	Parameters	Cu <sup>2+</sup>
Langmuir	$q_{max} (mg g^{-1})$	40.816
	$K_L (Lmg^{-1})$	0.806
	$R_L$	0.012
	$R^2$	0.966
Freundlich	$k_f$	15.488
	$1/n$	0.351
	$n$	2.853
	$R^2$	0.874
Temkin	$b_T (J mol^{-1})$	$4.501 \times 10^{-8}$
	$B (Lg^{-1})$	6.2863
	$A_T (Lg^{-1})$	$4.501 \times 10^8$
	$R^2$	0.937
DRK	$q_d$	32.769
	$A_{DRK}$	-6.008
	$E(KJ/mol)$	9.128
	$R^2$	0.961
Halsey	$1/n$	0.3505
	$N$	2.853
	$K$	2484.157
	$R^2$	0.874
Harkin-Jura	$A$	81.3008
	$B$	0.9675
	$R^2$	0.533

**Table 5: Thermodynamic parameters for adsorption of  $\text{Cu}^{2+}$  onto nZVI**

T (K)	$\Delta G(\text{kJ mol}^{-1})$	$\Delta H (\text{kJ mol}^{-1})$	$\Delta S (\text{J mol}^{-1} \text{ K}^{-1})$	Ka
298	6.31409	53.44925	200.4323	12.782
308	8.146.56			24.065
318	10.4076			51.204